

Citation for published version:

Collins, LR, Rajabi, NA, MacGregor, SA, Mahon, MF & Whittlesey, MK 2016, 'Experimental and computational studies of the copper borate complexes [(NHC)Cu(HB₃Et₃)] and [(NHC)Cu(HB(C₆F₅)₃)]', *Angewandte Chemie-International Edition*, vol. 55, no. 50, pp. 15539-15543. <https://doi.org/10.1002/anie.201608081>

DOI:

[10.1002/anie.201608081](https://doi.org/10.1002/anie.201608081)

Publication date:

2016

Document Version

Peer reviewed version

[Link to publication](https://doi.org/10.1002/anie.201608081)

This is the peer reviewed version of the following article: Dr. Lee R. Collins Nasir A. Rajabi Prof. Stuart A. Macgregor Dr. Mary F. Mahon Prof. Michael K. Whittlesey (2016) Experimental and Computational Studies of the Copper Borate Complexes [(NHC)Cu(HB₃Et₃)] and [(NHC)Cu(HB(C₆F₅)₃)]. *Angewandte Chemie International Edition*, 55(50), which has been published in final form at 10.1002/anie.201608081. This article may be used for non-commercial purposes in accordance with Wiley Terms and Conditions for Self-Archiving.

University of Bath

Alternative formats

If you require this document in an alternative format, please contact:
openaccess@bath.ac.uk

General rights

Copyright and moral rights for the publications made accessible in the public portal are retained by the authors and/or other copyright owners and it is a condition of accessing publications that users recognise and abide by the legal requirements associated with these rights.

Take down policy

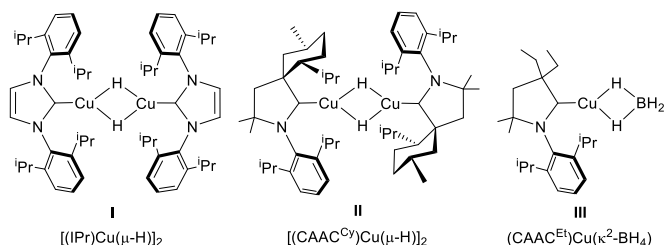
If you believe that this document breaches copyright please contact us providing details, and we will remove access to the work immediately and investigate your claim.

Experimental and Computational Studies of the Novel Copper Borate Complexes [(NHC)Cu(HBR₃)] (R = Et, C₆F₅)

Lee R. Collins,^[a] Nasir A. Rajabi,^[b] Stuart A. Macgregor,^{*,[b]} Mary F. Mahon^[a] and Michael K. Whittlesey^{*,[a]}

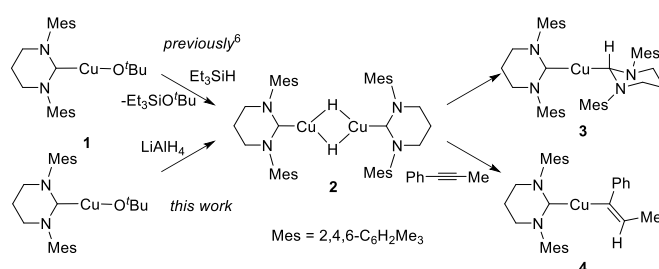
Abstract: The synthesis of the Cu-borate complexes [(6Mes)Cu(HBR₃)] featuring the unusual [HBEt₃][−] (**5**) and [HB(C₆F₅)₃][−] (**6**) ligands is described. Experimental and computational studies show both compounds feature a direct Cu–H interaction, but that while **5** is two-coordinate, **6** displays an additional, stabilizing Cu–C_{ipso}(C₆F₅) interaction.

There is considerable interest in mononuclear copper hydride species because of their proposed importance as intermediates in copper-catalyzed reductive transformations.^[1] However, simple mononuclear [LCuH] complexes (L = phosphine, N-heterocyclic carbene (NHC)) remain hitherto unknown: for L = PR₃, species ranging from dimers up to octanuclear clusters have been characterized,^[1h,2] while even very bulky NHCs still give only dimers (**I** and **II**, Scheme 1).^[3] The nearest example to an isolable mononuclear [LCuH] species reported to date is the three-coordinate [(CAAC^{Et})Cu(κ²-BH₄)] complex **III**.^[4,5] Herein, we report that during efforts to prepare mononuclear Cu–H species, we have instead isolated and structurally characterized two new examples of mononuclear copper borate complexes featuring the highly unusual borate ligands [HBEt₃][−] and [HB(C₆F₅)₃][−].



Scheme 1. Cu–H complexes prepared using IPr and CAAC ligands.

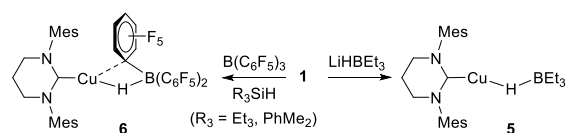
In recent work attempting to prepare [LCuH] species stabilized by large six-membered ring carbenes (e.g. from the reaction of **1** with tertiary silanes, Scheme 2), we showed that migratory insertion (MI) products such as **3** formed under mild conditions.^[6] This MI process thwarted efforts to spectroscopically characterize any putative Cu–H intermediates (e.g. **2**); however, Cu–H formation was implied through trapping with alkyne to give **4**.



Scheme 2. Synthesis and reactivity of [(6Mes)Cu(μ-H)]₂ (**2**).

We have now probed the reaction of **1** with alternative hydride sources. Addition of LiAlH₄ to a THF solution of **1** at room temperature brought about the instantaneous formation of a yellow solution, indicative of a Cu–H-containing species. Within minutes, this yellow color faded and Cu metal was deposited. A ¹H NMR spectrum of the solution showed that **3** was the major species present. However, when LiAlH₄ addition was carried out at 178 K, the Cu–H product (**2**) proved to be stable. DOSY measurements showed that it was dimeric (Scheme 2).^[7,8] The complex exhibited a low frequency Cu–H resonance at δ = 0.96 ppm, in good agreement with the shifts recently reported for [(6/7Dipp)Cu(μ-H)]₂ species.^[3d,9] However, whereas [(6/7Dipp)Cu(μ-H)]₂ prove stable for days at 298 K, **2** was stable only below 209 K. Above this temperature, the ¹H NMR resonances began to broaden and at 255 K signals for **3** were present.^[10]

Upon reacting (178 K) **1** with LiHBEt₃ instead of LiAlH₄, the rapid appearance of a yellow solution was again observed, but now resulting from the new monomeric complex [(6Mes)Cu(HBEt₃)] (**5**, Scheme 3) which features an intact {HBEt₃} moiety. The formation of **5** was unexpected since [HBEt₃][−] typically acts as a potent hydride source; indeed **II** was prepared from [(CAAC^{Cy})Cu(OtBu)] and LiHBEt₃.^[3b] Unsurprisingly, examples of isolable triethyl-borohydride complexes are rare, being confined to very electropositive metals.^[11]



Scheme 3. Synthesis of [(6Mes)Cu(HBR₃)] complexes **5** and **6**.

The X-ray structure of **5** (Figure 1) showed the presence of a two-coordinate Cu centre attached to the carbene and a monodentate {HBEt₃} moiety. The hydrogen atom on B(1) was located and refined without restraint, yielding C₆Mes–Cu–H and Cu–H–B angles of 162.4(13)

[a] Dr L. R. Collins, Dr M. F. Mahon, Prof. M. K. Whittlesey
Department of Chemistry, University of Bath, Claverton Down, Bath,
BA2 7AY, UK. E-mail: m.k.whittlesey@bath.ac.uk

[b] Mr N. A. Rajabi, Prof. S. A. Macgregor
Institute of Chemical Sciences, Heriot Watt University, Edinburgh,
EH14 4AS, UK. E-mail: S.A.Macgregor@hw.ac.uk
Supporting information for this article is given via a link at the end of
the document.

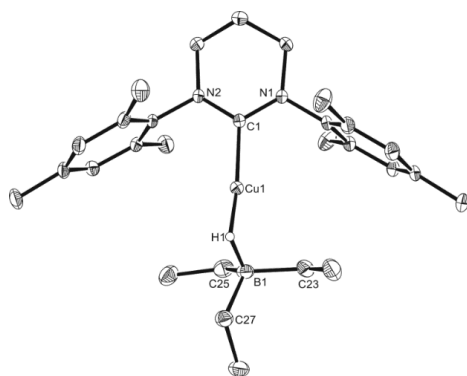


Figure 1. Molecular structure of **5**. Ellipsoids are shown at the 30% level. Hydrogen atoms (except for Cu-H-B) are removed for clarity.

and $110.2(18)^\circ$, respectively, and B-H and Cu-H distances of 1.22(3) and 1.56(3) Å, respectively. The latter is comparable to the shortest Cu-H distance in **II**,^[3b] but much shorter than either of the Cu-H bond lengths in **III** (1.679(2) Å, 1.717(18) Å). Additional characterization of **5** was performed in solution at low temperature (209 K). The ^1H NMR spectrum featured a broad, low frequency signal (relative integral of 1) at $\delta = -2.60$ ppm, assigned to the Cu-H. The ^1H coupled ^{13}C NMR spectrum showed a 12 Hz doublet splitting of the carbenic carbon resonance ($\delta = 202$ ppm), confirming $\text{C}_{6\text{Mes}}\text{-Cu-H}$ connectivity.

The nature of the $\{\text{Cu-H-BEt}_3\}$ interaction in **5** was assessed via Quantum Theory of Atoms in Molecules (QTAIM) and Natural Bond Orbital (NBO) analyses using the BP86 functional and geometries based on the crystallographically determined structure.^[12] The QTAIM molecular graph (Figure 3(a)) identifies Cu-H and B-H bond paths, as well as one for the $\text{Cu-C}_{6\text{Mes}}$ bond. No further bonding interactions involving Cu (e.g. to any atoms of the Et substituents) are seen, thereby supporting the assignment of **5** as a two-coordinate complex.

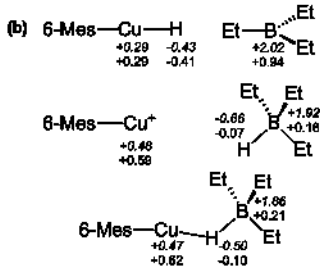
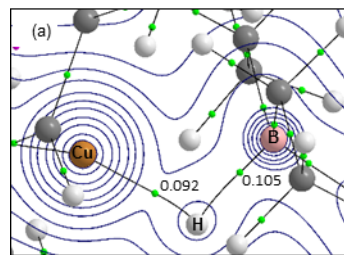


Figure 3. (a) Detail of the QTAIM molecular graph of **5** showing electron density contours in the $\{\text{Cu/H/B}\}$ plane. Bond critical points (BCPs) are shown as green spheres and key values of $\rho(r)$ (the associated BCP electron densities) are indicated in au. (b) Computed atomic charges for **5** and selected comparator species (QTAIM charges in italics; NBO charges in plain text). Full QTAIM metrics are provided in the ESI, along with equivalent $\rho(r)$ values obtained with a range of different functionals.

Figure 3(b) shows the computed QTAIM and NBO charges at the Cu, H and B centres in **5**, the BP86-optimized free $[(6\text{Mes})\text{Cu}]^+$ and $[\text{HBEt}_3]^-$ ions as well as the neutral $[(6\text{Mes})\text{CuH}]$ and BEt_3 species. Significantly, the charge distribution in **5** more closely resembles that in the free ions, rather than the neutral species. NBO analysis also highlights a $\sigma_{\text{B-H}} \rightarrow \text{Cu}$ donation that a 2nd order perturbation analysis quantifies at 67.1 kcal/mol (see Figure S23 for NBO plots). The computed evidence therefore indicates that **5** is a borate complex of a $\{(6\text{Mes})\text{Cu}\}^+$ fragment, rather than a Lewis acid-stabilized Cu-hydride (viz. $[(6\text{Mes})\text{CuH}\cdots\text{BEt}_3]$).

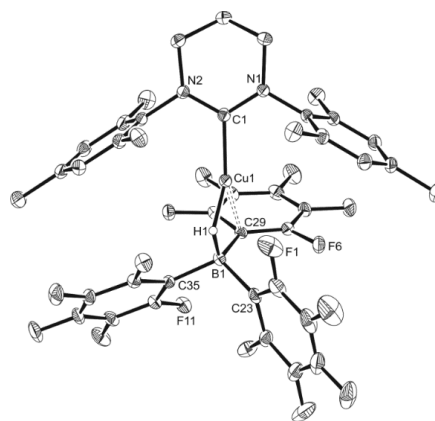


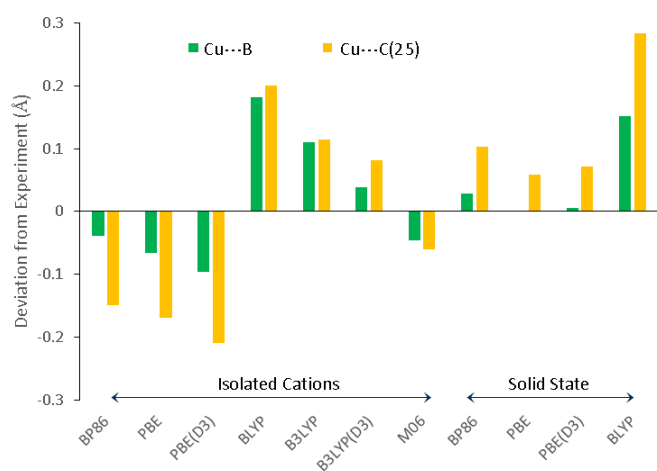
Figure 2. Molecular structure of **6**. Ellipsoids are shown at the 30% level. Hydrogen atoms (except for Cu-H-B) are removed for clarity.

Experimentally, complex **5** was found to be stable both in THF solution and the solid state for several days below ca. 243 K, but started to decompose within hours upon warming above this temperature through B-H bond cleavage (apparent from the appearance of BEt_3 (^{11}B : $\delta = 73$ ppm)).^[11c] **3** and H_2 were also formed, alongside deposition of Cu metal. Interestingly, in contrast to the quantitative formation of the migratory insertion product **3** from **2** (Scheme 1), **5** converted at room temperature to **3** in only ca. 5% yield due to the transformation of $[\text{HBEt}_3]^-$ to $[\text{BEt}_4]^-$ and $[\text{H}_2\text{BEt}_2]^-$.^[13] This resulted in the formation of the $[\text{BEt}_4]^-$ salt of the known bis-carbene cation, $[(6\text{Mes})_2\text{Cu}]^+$ (ESI), and a second species believed to be $[(6\text{Mes})\text{Cu}(\text{H}_2\text{BEt}_2)]$ as the ultimate products of the reaction.

The formation of **5** and its formulation as a Cu-borate complex prompted us to consider the formation of related species with properties modulated by the nature of the B-substituents. Taking a lead from the reactions of *s*-block, early transition metal and lanthanide complexes with Lewis acidic boranes,^[14] **1** was treated with R_3SiH in the presence of $\text{B}(\text{C}_6\text{F}_5)_3$. A rapid reaction ensued in the case of Et_3SiH to give a mixture of $[(6\text{Mes})\text{Cu}(\text{HB}(\text{C}_6\text{F}_5)_3)]$ (**6**) and $[(6\text{Mes})_2\text{Cu}][\text{B}(\text{C}_6\text{F}_5)_4]^-$ (**7**) (ESI).^[15] Use of PhMe_2SiH rather than Et_3SiH gave only **6**. An X-ray crystal structure (Figure 2) showed that **6** was mononuclear like **5**, but that, in addition to a Cu-H interaction, there was also one short $\text{Cu-C}_{\text{ipso}}$ contact (2.2183(17) Å) to the C_6F_5 ring based on C29.^[16] The nature of this interaction differs noticeably from those found with more electropositive metals, which invariably involve *ortho*-C-F bond contacts. In particular, the $\text{Cu-C}_{\text{ipso}}$ interaction in **6** was seen to be concomitant with lengthening of the B(1)-C(29) distance to 1.657(3) Å, relative to the B(1)-C(23) and B1-C(35) distances of 1.624(3) and 1.628(3) Å, respectively. Additionally, the $\text{C}_{6\text{Mes}}\text{-Cu-H}$ angle of $146.5(8)^\circ$ in **6** is notably more acute than that observed in **5** ($162.8(14)^\circ$). The Cu-H and B-H distances are each comparatively similar in both structures.

6 was more thermally stable than **5** and could be characterized at room temperature. The ^{11}B NMR spectrum showed a resonance at $\delta = -28.1$ ppm, slightly upfield of the ion-separated species $[\text{X}][\text{HB}(\text{C}_6\text{F}_5)_3]$ ($\text{X} = \text{P}^t\text{Bu}_3\text{H}$, $\delta = -25.5$ ppm;^[17a] NBu_4 , $\delta = -25.4$ ppm).^[17b] Moreover, the $^1\text{J}(\text{B,H})$ doublet splitting in **6** was smaller (60 Hz) than in either of these compounds (100 and 82 Hz, respectively) or any of the early metal complexes (e.g. $[(\text{C}(\text{SiMe}_2\text{H})_3)\text{M}(\text{THF})_2(\text{HB}(\text{C}_6\text{F}_5)_3)]$, $\text{M} = \text{Ca}$: 76 Hz; $\text{M} = \text{Yb}$: 73 Hz),^[14c] suggestive of a significant Cu-H-B interaction. This was supported by IR spectroscopy ($\nu(\text{B-H})$: 2361 cm^{-1})^[14c] and the ^{19}F NMR chemical shift difference of 5.4 Hz between the *meta*- and *para*-fluorine atoms.^[18] Although we could not observe the Cu-H resonance directly in the ^1H NMR spectrum, ^1H - ^{11}B HMQC spectroscopy revealed it at $\delta = 2.08$ ppm. Over ca. 12 h in solution, **6** degraded to **7** and deposited metallic Cu.

The QTAIM molecular graph for **6** (Figure 4(a)) confirmed the presence of Cu-H and H-B bond paths. Compared to **5**, the Cu-H BCP has a lower $\rho(r)$ (0.083 au, *cf.* 0.092 au) indicating a weaker interaction, and this is complemented by the higher $\rho(r)$ of the B-H BCP (0.135 au, *cf.* 0.105 au). Weaker donation to Cu in **6** is also manifest in a higher computed positive charge at Cu (Figure 4(b)) and the reduced $\sigma_{B-H} \rightarrow$ Cu interaction which the NBO 2nd order perturbation analysis quantifies as 42.9 kcal/mol. The similar charges at Cu, B and H in **6** and free [(6Mes)Cu]⁺ and [HB(C₆F₅)₃]⁻ ions again suggest **6** is a borate complex. An additional feature, again consistent with a more electron deficient Cu centre, is the presence of a Cu-C_{ipso} bond path which entails a ring critical point associated with the {CuHBC_{ipso}} unit. The lower value of $\rho(r)$ at the Cu-C_{ipso} BCP (0.055 au) indicates a weaker interaction than the Cu-H bond and the NBO 2nd order perturbation analysis confirms this, providing an interaction energy of only 7.1 kcal/mol corresponding to donation from the C_{ipso}-B σ -bond to Cu. NBO also suggests an



additional stabilization occurs via donation from one of the C_{ipso}-C_{ortho} bonds of the C₆F₅ ring ($\Delta E = -7.9$ kcal/mol, see Figure S24).

Figure 4. (a) Detail of the QTAIM molecular graph for **6** showing electron density contours for the {Cu/H/B plane}. Bond critical points (BCPs) and ring critical points (RCPs) are shown as green and magenta spheres respectively and $\rho(r)$ values of key CPs are indicated in au. (b) Computed atomic charges for **6** and selected comparator species (QTAIM charges in *italics*; NBO charges in plain text). Full QTAIM metrics are provided in the ESI along with equivalent $\rho(r)$ values obtained with a range of different functionals..

Reproducing the molecular geometries of **5** and **6** presented a challenge to theory; in particular the structure of the {Cu(HBEt₃)} moiety in **5** was very sensitive to functional choice. Given this, we also investigated the role of the chemical model used in the calculations by computing the extended solid-state structure of **5** with periodic DFT calculations. Such an approach has been shown to be important in correctly describing ambiguous bonding situations.^[19] Figure 5 shows deviations from experiment for the Cu...B and Cu...C(25) distances computed in **5** with different functionals, where the latter is a proxy for any additional Cu...H interactions involving the Et substituents. For the molecular calculations, BP86 provides the best agreement for the Cu...B distance, but underestimates Cu...C(25) by 0.15 Å. PBE gives somewhat poorer agreement, and this deteriorates further with PBE(D3), i.e. when a dispersion correction is included in the optimization. These geometries imply the presence of a Cu...H-C(25) agostic interaction and thus a three-coordinate Cu centre, at odds with the observed two-coordinate geometry. In contrast, BLYP and B3LYP overestimate both distances, a result that has parallels in the description of agostic interactions.^[20] B3LYP(D3) improves the situation but this relatively

good net performance probably reflects a cancellation of errors, due to the poor B3LYP geometry and an overestimation of intramolecular dispersion effects in the isolated molecular model. Of these molecular calculations, M06 provides the best overall result, with both Cu...B and Cu...C(25) being underestimated by ca. 0.05 Å. A wider comparison of computed structural metrics is provided in the Supporting Information.

Full optimization of the extended solid-state structure of **5** under periodic boundary conditions with BP86 and (particularly) PBE provided improved geometries; moreover, the results are now far less sensitive to the inclusion of dispersion, reflecting how the full solid-state environment can balance the intramolecular dispersion that was overestimated in the calculations using molecular models. Use of an extended model does not guarantee good agreement, however, with BLYP still giving a poor geometry, even with the solid-state model. An equivalent set of calculations was performed for **6** and similar trends were obtained. In this case, the stronger Cu-C_{ipso} interaction makes the computed geometries less functional dependent, although B3LYP significantly overestimates both Cu-C_{ipso} and Cu...B distances. Geometries derived from the periodic calculations are now in good agreement with experiment (see Figure S22).

Figure 5. Cu...B and Cu...C(25) distances in **5** computed with various functionals and displayed as deviations from the experimental values of 2.283(3) Å and 2.619(3) Å respectively. Calculations employed either the isolated molecule (Gaussian) or the extended solid state via periodic boundary conditions (CP2K).

The isolation of the [HBEt₃]⁻ adduct **5** contrasts with the [(CAAC^{Cy})Cu(HBEt₃)] analogue that is (presumably) present as an (unseen) intermediate *en route* to **II** (Scheme 1). We have assessed the stabilities of these species, along with **6** and [(CAAC^{Et})Cu(κ^2 -BH₄)] (**III**) by computing the free energy changes associated with borane loss and dimerization (Figure 6). These indicate a significantly stronger H-B(C₆F₅)₃ bond in **6** ($\Delta G_1 = +38.2$ kcal/mol) compared to the H-BEt₃ bond in **5** ($\Delta G_1 = +10.8$ kcal/mol). **5** may therefore be susceptible to BEt₃ loss to form [(6Mes)CuH], however, dimer formation is not thermodynamically accessible in this case ($\Delta G_3 = +6.8$ kcal/mol), and so alternative decomposition routes are apparently accessed, as seen experimentally. The BH₃ moiety in **III** is also strongly bound ($\Delta G_1 = +36.9$ kcal/mol), consistent with the isolation of the borohydride complex.^[4] In contrast, BEt₃ loss from [(CAAC^{Cy})Cu(HBEt₃)] is particularly facile ($\Delta G_1 = +5.8$ kcal/mol) and the subsequent dimerization energy is sufficiently exergonic to rationalize the formation of dimer **II** upon reaction of [(CAAC^{Cy})Cu(O'Bu)] with LiHBEt₃.^[3b]

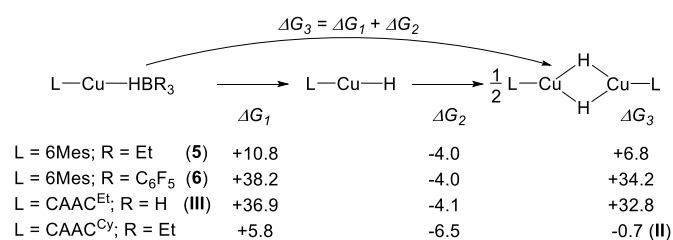


Figure 6. Computed free energy changes (kcal/mol; BP86-optimised with corrections for dispersion (D3) and THF solvent) for borane loss and dimerization of different [LCu(HBR₃)] complexes.

The computational findings that **5** and **6** are not simple Lewis acid stabilized forms of [(6Mes)CuH] were reinforced by probing their reactivity with PhC≡CMe. In neither case was the hydrocupration product **4** (Scheme 1) formed. Addition of PhC≡CMe (2 equiv) to **5** at 225 K resulted in no reaction until ca. 288 K, at which point the presence of multiplets in the $\delta = 4$ –6 ppm region of the ¹H NMR spectrum suggested that some reduction of the alkyne had occurred. However, none of the signals matched those of **4**.^[6] The ¹¹B NMR spectrum showed resonances at $\delta = 60$, 52 and -14 ppm suggestive of multiple boron-containing species being produced. There was no reaction between **6** and the alkyne over days at room temperature, with only the transformation to the homoleptic cationic bis-carbene complex **7** apparent from the ¹¹B NMR spectrum.

In conclusion, the synthesis of the novel Cu-borate complexes [(6Mes)Cu(HBR₃)] (R = Et (**5**), C₆F₅ (**6**)) has been reported. Experimental and computational studies show that **5** features a two-coordinate Cu centre, while **6** exhibits a further stabilizing Cu–C_{ipso} interaction to one C₆F₅ substituent. Although both species possess a direct Cu–H interaction, neither can be considered as Lewis acid stabilized forms of [(6Mes)CuH]. The isolation of a monomeric [(NHC)CuH] species, therefore, still remains an elusive target.

Acknowledgements

We thank the University of Bath (DTA to LRC) and Heriot-Watt University (James Watt scholarship to NAR) for financial support and Prof Gregory Wildgoose (University of East Anglia) for discussions and experimental assistance. This work used the ARCHER UK National Supercomputing Service (<http://www.archer.ac.uk>).

Keywords: heterocyclic carbene • copper • hydride ligand • Lewis acids • DFT calculations

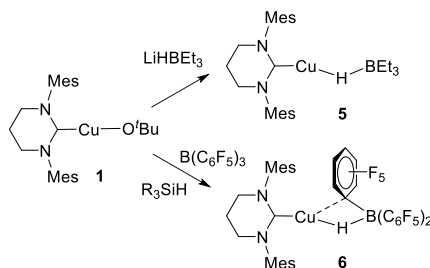
- [1] a) C. Deutsch, N. Krause, B. H. Lipshutz, *Chem. Rev.* **2008**, *108*, 2916–2927; b) T. Fujihara, T. H. Xu, K. Semba, J. Terao, Y. Tsuji, *Angew. Chem.* **2011**, *123*, 543–547; *Angew. Chem. Int. Ed.* **2011**, *50*, 523–527; c) A. M. Whittaker, G. Lalic, *Org. Lett.* **2013**, *15*, 1112–1115; d) N. Cox, H. Dang, A. M. Whittaker, G. Lalic, *Tetrahedron* **2014**, *70*, 4219–4231; e) T. Vergote, F. Nagra, A. Merschaert, O. Riant, D. Peeters, T. Leyssens, *Organometallics* **2014**, *33*, 1953–1963; f) M. R. Uehling, A. M. Suess, G. Lalic, *J. Am. Chem. Soc.* **2015**, *137*, 1424–1427; g) S.-L. Shi, S. L. Buchwald, *Nat. Chem.* **2015**, *7*, 38–44; h) A. J. Jordan, G. Lalic, J. P. Sadighi, *Chem. Rev.* **2016**, *116*, 8318–3372.

- [2] a) S. A. Bezman, M. R. Churchill, J. A. Osborn, J. Wormald, *J. Am. Chem. Soc.* **1971**, *93*, 2063–2065; b) T. H. Lemmen, K. Folting, J. C. Huffman, K. G. Caulton, *J. Am. Chem. Soc.* **1985**, *107*, 7774–7775; c) G. V. Goeden, J. C. Huffman, K. G. Caulton, *Inorg. Chem.* **1986**, *25*, 2484–2485; d) C. F. Albert, P. C. Healy, J. D. Kildea, C. L. Raston, B. W. Skelton, A. H. White, *Inorg. Chem.* **1989**, *28*, 1300–1306.
- [3] a) N. P. Mankad, D. S. Laitar, J. P. Sadighi, *Organometallics* **2004**, *23*, 3369–3371; b) G. D. Frey, B. Donnadieu, M. Soleilhavoup, G. Bertrand, *Chem. Asian J.* **2011**, *6*, 402–405; c) S. C. Schmid, R. Van Hoveln, J. W. Rigoli, J. M. Schomaker, *Organometallics* **2015**, *34*, 4164–4173; d) A. J. Jordan, C. M. Wyss, J. Bacsá, J. P. Sadighi, *Organometallics* **2016**, *35*, 613–616. See also: e) C. M. Wyss, B. K. Tate, J. Bacsá, T. G. Gray, J. P. Sadighi, *Angew. Chem.* **2013**, *125*, 13158–13161; *Angew. Chem. Int. Ed.* **2013**, *52*, 12920–12923.
- [4] X. Hu, M. Soleilhavoup, M. Melaimi, J. Chu, G. Bertrand, *Angew. Chem. Int. Ed.* **2015**, *54*, 6008–6011.
- [5] The stability of **III** contrasts markedly with that of the phosphine analogue [(PPh₃)Cu(κ²-BH₄)]. R. K. Hertz, R. Goetze, Shore, *Inorg. Chem.* **1979**, *18*, 2813–2816.
- [6] L. R. Collins, I. M. Riddlestone, M. F. Mahon, M. K. Whittlesey, *Chem. Eur. J.* **2015**, *21*, 14075–14084.
- [7] References ^[3a,3c,d] provide examples which associate yellow colored solutions with [(NHC)Cu(μ-H)]₂ dimers.
- [8] DOSY measurements gave a value for τ_H of 6.2 Å. Based on previous studies of diamidocarbene copper chloride complexes (L. R. Collins, J. P. Lowe, M. F. Mahon, R. C. Poulten, M. K. Whittlesey, *Inorg. Chem.* **2014**, *53*, 2699–2707), the value is consistent with a dimeric structure.
- [9] 6Dipp = 1,3-bis(2,6-diisopropylphenyl)-3,4,5,6-tetrahydropyrimidin-2-ylidene; 7Dipp = 1,3-bis(2,6-diisopropylphenyl)-4,5,6,7-tetrahydro-1,3-diazepin-2-ylidene.
- [10] All attempts to isolate **2** were unsuccessful. On occasion, crystalline material was isolated (ESI), but this proved to be [(6Mes)AlH₃].
- [11] a) D. Baudry, A. Dormond, B. Lachot, M. Visseaux, G. Zucchi, *J. Organomet. Chem.* **1997**, *547*, 157–165; b) M. J. Harvey, T. P. Hanusa, M. Pink, *Chem. Commun.* **2000**, 489–490; c) F. Basuli, J. Tomaszewski, J. C. Huffman, D. J. Mindiola, *Organometallics* **2003**, *22*, 4705–4714; d) W. J. Evans, J. M. Perotti, J. W. Ziller, *Inorg. Chem.* **2005**, *44*, 5820–5825; e) D. M. Lyubov, G. K. Fukin, A. A. Trifonov, *Inorg. Chem.* **2007**, *46*, 11450–11456; f) S. Kriek, H. Görls, M. Westerhausen, *Inorg. Chem. Comm.* **2010**, *13*, 1466–1469; g) X. W. Zhang, G. H. Maunders, S. Gießmann, R. MacDonald, M. J. Ferguson, A. H. Bond, R. D. Rogers, A. Sella, J. Takats, *Dalton Trans.* **2011**, *40*, 195–210.
- [12] Calculations on the isolated cations within **5** and **6** were run with Gaussian 09 while periodic DFT calculations were performed with CP2K. See ESI for full details.
- [13] M. G. Crestani, M. Muñoz-Hernández, A. Arévalo, A. Acosta-Ramírez, J. J. García, *J. Am. Chem. Soc.* **2005**, *127*, 18066–18073.
- [14] a) W. J. Evans, K. J. Forrestal, M. A. Ansari, J. W. Ziller, *J. Am. Chem. Soc.* **1998**, *120*, 2180–2181; b) K. Yan, B. M. Upton, A. Ellern, A. D. Sadow, *J. Am. Chem. Soc.* **2009**, *131*, 15110–15111; c) K. Yan, G. Schoendorff, B. M. Upton, A. Ellern, T. L. Windus, A. D. Sadow, *Organometallics* **2013**, *32*, 1300–1316; d) M. D. Anker, M. Arrowsmith, P. Bellham, M. S. Hill, G. Kociok-Köhn, D. J. Liptrot, M. F. Mahon, C. Weetman, *Chem. Sci.* **2014**, *5*, 2826–2830; e) N. L. Lampland, A. Pindwal, S. R. Neal, S. Schlauderer, A. Ellern, A. D. Sadow, *Chem. Sci.* **2015**, *6*, 6901–6907.
- [15] L. R. Collins, T. M. Rookes, M. F. Mahon, I. M. Riddlestone, M. K. Whittlesey, *Organometallics* **2014**, *33*, 5882–5887.
- [16] A gold analogue of **6** has been spectroscopically identified in the reaction of [(6/7Dipp)AuH] with B(C₆F₅)₃. N. Phillips, T. Dodson, R. Tiffin, J. I. Bates, S. Aldridge, *Chem. Eur. J.* **2014**, *20*, 16721–16731.
- [17] a) G. C. Welch, D. W. Stephan, *J. Am. Chem. Soc.* **2007**, *129*, 1880–1881; b) E. J. Lawrence, V. S. Oganessian, D. L. Hughes, A. E. Ashley, G. G. Wildgoose, *J. Am. Chem. Soc.* **2014**, *136*, 6031–6036.
- [18] A. D. Horton, J. de With, *Organometallics* **1997**, *16*, 5424–5436.
- [19] J. Moellmann, S. Grimme, *Organometallics* **2013**, *32*, 3784–3787.
- [20] D. A. Pantazis, J. E. McGrady, F. Maseras, M. Etienne, *J. Chem. Theory Comput.* **2007**, *3*, 1329–1336.

Copper Borates

Lee R. Collins, Nasir A. Rajabi, Stuart A. Macgregor,* Mary F. Mahon and Michael K. Whittlesey* _____
Page – Page

Experimental and Computational Studies of the Novel Copper Borate Complexes $[(\text{NHC})\text{Cu}(\text{HBR}_3)]$ ($\text{R} = \text{Et}$, C_6F_5)



*Unusual Cu-borate complexes $[(6\text{Mes})\text{Cu}(\text{HBR}_3)]$ ($\text{R} = \text{Et}$ (**5**), C_6F_5 (**6**)) are described. Experimental and computational studies show both species exhibit a direct Cu-H interaction with **5** featuring a two-coordinate Cu while **6** has a further Cu- C_{ipso} interaction to one C_6F_5 substituent.*